




Article

The Effect of High-Temperature Annealing on the Magnetic and Structural Properties of (MnFePSi)-Based Glass-Coated Microwires

Mohamed Salaheldeen ^{1,2,3,*} , Valentina Zhukova ^{1,2,4} , Julian Gonzalez ^{1,2} and Arcady Zhukov ^{1,2,4,5,*} 

¹ Department of Polymers and Advanced Materials, Faculty of Chemistry, University of the Basque Country, UPV/EHU, 20018 San Sebastián, Spain; valentina.zhukova@ehu.eus (V.Z.); julianmaria.gonzalez@ehu.eus (J.G.)

² Department of Applied Physics I, EIG, University of the Basque Country, UPV/EHU, 20018 San Sebastián, Spain

³ Physics Department, Faculty of Science, Sohag University, Sohag 82524, Egypt

⁴ EHU Quantum Center, University of the Basque Country, UPV/EHU, 20018 San Sebastián, Spain

⁵ IKERBASQUE, Basque Foundation for Science, 48011 Bilbao, Spain

* Correspondence: mohamed.salaheldeenmohamed@ehu.eus (M.S.); arkadi.joukov@ehu.eus (A.Z.)

Abstract: In this paper, the impact of annealing at different temperatures (973 K, 1073 K, and 1123 K for 1 h) on the magnetic and microstructural properties of MnFePSi-based glass-coated microwires is studied. Annealing significantly influences the magnetic and microstructural properties of Mn–Fe–P–Si glass-coated microwires. XRD analysis reveals that increasing the annealing temperature leads to a notable increase in the Fe₂P phase content, reaching a maximum at 1123 K, while simultaneously reducing the presence of secondary phases observed in the as-prepared sample. The reduction in secondary phases in Mn–Fe–P–Si-based microwires, grain size, and internal stress relaxation have a profound impact on their magnetic behavior. High coercivity values are observed in both the as-prepared and annealed samples. However, annealing at higher temperatures (1073 K and 1123 K) results in a significant reduction in coercivity, decreasing from 1200 Oe for the sample annealed at 973 K to 300 Oe and 150 Oe, respectively. In addition, the sample annealed at 1123 K for 1 h shows a notable paramagnetic behavior for loops measured from 200 K to 300 K. Meanwhile, the other samples show ferromagnetic behavior for all measured temperatures from 5 to 300 K. This study highlights the significant potential for tailoring and modifying various magnetic properties of Mn–Fe–P–Si glass-coated microwires, including metamagnetic phase transitions, magnetic behavior, and the control of magnetic response (hardness/softness). Such tailored properties make Mn–Fe–P–Si glass-coated microwires promising candidates for a wide range of applications.

Keywords: Mn–Fe–P–Si alloys; glass-coated microwires; Taylor–Ulitsky technique; annealing; XRD analysis



Academic Editors: Erdem Karakulak and Marzena Lachowicz

Received: 28 February 2025

Revised: 22 March 2025

Accepted: 25 March 2025

Published: 27 March 2025

Citation: Salaheldeen, M.; Zhukova, V.; Gonzalez, J.; Zhukov, A. The Effect of High-Temperature Annealing on the Magnetic and Structural Properties of (MnFePSi)-Based Glass-Coated Microwires. *Crystals* **2025**, *15*, 311. <https://doi.org/10.3390/cryst15040311>

Copyright: © 2025 by the authors. Licensee MDPI, Basel, Switzerland. This article is an open access article distributed under the terms and conditions of the Creative Commons Attribution (CC BY) license (<https://creativecommons.org/licenses/by/4.0/>).

1. Introduction

In recent years, the continuous development of magnetic micro- and nanostructures has significantly advanced both fundamental scientific research and technological applications [1–5]. Unlike bulk magnetic materials, the systematic engineering of micro- and nanomaterials has led to groundbreaking advances in areas such as the fabrication of magnetic micro- and nanostructures with tailorable physical properties, the exploration of multidimensional magnetic properties in magnetic micro- and nanostructures, and their

prospective applications [3–5]. In addition, precise control over the grain size, morphology, and phase content of magnetic micro- and nanostructures is of paramount importance in determining their unique physical and chemical properties, which are essential for potential applications [6,7].

Magnetic materials engineered at the micro- and nanoscale, which exhibit thermoelastic martensitic phase transitions, have garnered significant research interest due to their unique properties [8–31]. These materials have a distinctive synergy of functions, presenting great opportunities for technological advancement. Prominent features encompass shape memory (SM), giant superelasticity (GS), magnetic field-induced strain (MFIS), and elastocaloric and magnetocaloric (EMC) effects [2,4,5,8–34].

In recent decades, there has been a surge of research dedicated to magnetocaloric materials, which serve as essential components in magnetic refrigeration systems [2,4,5,11]. Despite their potential, existing refrigerators often operate at relatively low frequencies (up to a few Hz), hindering their overall cooling efficiency [35,36]. Theoretical investigations have indicated that the cooling efficiency of magnetic refrigerators can be significantly enhanced by optimizing the shape of the magnetocaloric materials employed [37–39]. Specifically, it has been theorized that magnetic materials composed of magnetocaloric microwires, such as Gd and NiMnGa wires, offers an optimal device configuration compared to powder or laminate structures [37–39]. The increased surface-to-volume ratio of magnetocaloric wires is expected to facilitate more efficient heat transfer between the magnetic refrigerant and the surrounding liquid.

Mn–Fe–P–Si alloys have emerged as promising magnetocaloric materials due to their substantial magnetocaloric effect near room temperature [40,41]. The low cost of these materials, which do not require expensive or critical elements, further enhances their appeal as viable candidates for large-scale cooling applications. MnFePSi alloys exhibit a hexagonal Fe₂P-type crystal structure (space group P6₂m) [42]. Within this structure, Mn and Fe atoms occupy specific sites: Mn atoms occupy pyramid-shaped sites (3g), while Fe atoms favor tetrahedral sites (3f) [42,43]. Neutron diffraction studies have elucidated the ferromagnetic (FM) state in these alloys, revealing the in-plane alignment of both Mn and Fe magnetic moments within the basal ab plane [43]. Density Functional Theory (DFT) simulations have further highlighted the unique mixed magnetism of Mn–Fe–P–Si, with Mn atoms maintaining a relatively constant magnetic ordering even above the critical temperature (T_c), while Fe atoms exhibit a significant increase in magnetic moment at T_c . The presence of Phosphorus (P) and Silicon (Si) atoms is crucial in enabling Fe atoms to develop a strong magnetic moment within Mn–Fe–P–Si alloys [43]. This combination of properties makes Mn–Fe–P–Si alloys highly promising for applications such as enhancing the efficiency of solid-state cooling systems and magnetic refrigeration technologies [44–49]. From a materials engineering perspective, achieving a high fraction of the desirable Fe₂P phase in Mn–Fe–P–Si alloys presents a significant challenge. Previous research has demonstrated that conventional methods often require prolonged heat treatment, spanning several days or months, at elevated temperatures to form a substantial volume fraction of the Fe₂P phase and ensure compositional homogeneity within Mn–Fe–P–Si materials [50–54]. Consequently, these production methods can lead to increased overall costs. The increasing push for smaller devices in modern technology, including magnetocaloric systems, has amplified the attractiveness of Mn–Fe–P–Si alloys [44–49,55–66]. A distinctive characteristic of Mn–Fe–P–Si lies in its versatility, allowing for its fabrication into various micro-scale structures, including particles, wires, ribbons, films, and complex layered configurations. The primary magnetic parameters of Mn–Fe–P–Si alloys, such as coercivity, thermomagnetic behavior, magnetic transitions, and Curie temperature, are significantly influenced by factors like chemical composition, annealing conditions, secondary phases, and fabrication techniques.

Consequently, a wide range of Curie temperatures, spanning from 100 K to 470 K, has been reported [19,44–49,55–67]. The fact that MnFePSi alloys can be easily shaped in various ways allows for a wide variety of potential uses [44–49,55–67].

Recently, we succeeded in fabricating Mn–Fe–P–Si microwires with Fe₂P as the main phase. Interesting magnetic behavior, such as a metastable magnetic phase transition, high coercivity, multistep magnetic behavior, and interesting thermomagnetic curves with different magnetic fields and temperatures, has been reported, which does not exist in the master bulk alloy [19,55,67].

Sub-micrometer diameter glass-coated microwires, have garnered significant attention due to their diverse applications, especially in the field of sensing technology [68,69]. These composite materials consist of a metallic nucleus coated by an insulating glass coating of micrometric thickness. Such a composite structure provides various advantages. Compared to other Mn–Fe–P–Si alloys, glass-coated Mn–Fe–P–Si microwires enable novel industrial applications [68,69]. Mn–Fe–P–Si microwires, unlike their bulk or thin-film counterparts, facilitate new applications in diverse industries [68,69]. The glass coating provides mechanical and anti-corrosion protection for the metallic nucleus, preventing electrical short circuits and enhancing corrosion resistance, thereby extending the microwire's lifespan. Moreover, the thickness of the glass coating can be precisely controlled during the manufacturing process to meet specific application requirements.

By systematically varying annealing conditions, we examined the magneto-structural properties of Mn–Fe–P–Si glass-coated microwires. The results indicate that annealing profoundly influences the microwires, leading to observable changes in coercivity, the formation of secondary phases, magnetic stability, thermomagnetic behavior, and microstructure. These findings underscore the heightened sensitivity of Mn–Fe–P–Si wires to thermal treatment compared to their bulk alloy counterparts. The material's responsive nature paves the way for the future exploration and development of applications utilizing metamagnetic phase transitions and bi-stable magnetic functionalities.

2. Materials and Methods

2.1. Fabrication of Bulk Mn–Fe–P–Si-Master Alloy

This study focuses on the fabrication and studies of thin, Mn–Fe–P–Si alloy glass-coated microwires. The fabrication process can be roughly divided into two main stages: the production of a bulk Mn–Fe–P–Si alloy ingot and the subsequent microwire preparation from this ingot. The first stage involves the meticulous production of a Mn₄₀Fe₃₀P₁₅Si₁₅ bulk alloy via ARC melting. The raw materials employed in the fabrication process consisted of high-purity crystals of manganese (Mn, ≥99.5%), iron (Fe, ≥99.99%), iron–phosphorus chunks (FeP, ≥98%), and silicon (Si, ≥99.999%). To compensate for potential manganese losses during the arc-melting process, an excess of 5 wt% of manganese was intentionally added to the initial mixture.

The powder mixture is then carefully transferred into a copper crucible specifically designed for high-temperature applications. The crucible is subsequently placed within a vacuum chamber filled with argon gas and subjected to an electric arc, inducing intense localized heat that melts the powder mixture. To ensure complete liquefaction and homogenization, the melting process is meticulously controlled. Upon complete melting, the electric arc is extinguished, and the molten metal is allowed to cool progressively under controlled atmospheric conditions. This controlled cooling promotes the formation of a uniform and homogenous Mn₄₀Fe₃₀P₁₅Si₁₅ bulk alloy ingot. To improve the uniformity of the alloy's internal structure and enhance its overall quality, the melting and homogenization process can be repeated multiple times, usually five cycles. Remelting contributes to refining the grain structure of the bulk alloy. Following solidification, the Mn₄₀Fe₃₀P₁₅Si₁₅

bulk alloy ingot undergoes comprehensive characterization to evaluate its structural and compositional properties. This characterization step is crucial for ensuring the quality and suitability of the bulk alloy for subsequent processing into microwires.

2.2. Preparation of Mn–Fe–P–Si Glass-Coated Microwires

Glass-coated microwires were fabricated using the Taylor–Ulitsky technique, with a Duran glass coating (Figure 1b–d). For further details regarding the fabrication process and experimental conditions, please refer to previous studies [19,55,67–73]. The fabricated microwires exhibited a total diameter of 28 μm , with a metallic core measuring 14.7 μm . Energy-dispersive X-ray spectroscopy (EDX) revealed the composition of $\text{Mn}_{40}\text{Fe}_{30}\text{P}_{15}\text{Si}_{15}$, with a minor 0.5% variation from the intended proportions, likely due to manganese loss during melting and wire formation. The as-prepared microwires were then annealed in a vacuum (2×10^{-4} Pa) at temperatures of 973 K, 1073 K, and 1123 K for one hour, using a heating rate of 10 K/min and furnace cooling. Post-annealing, EDX analysis was performed to determine if the heat treatment affected the chemical composition.

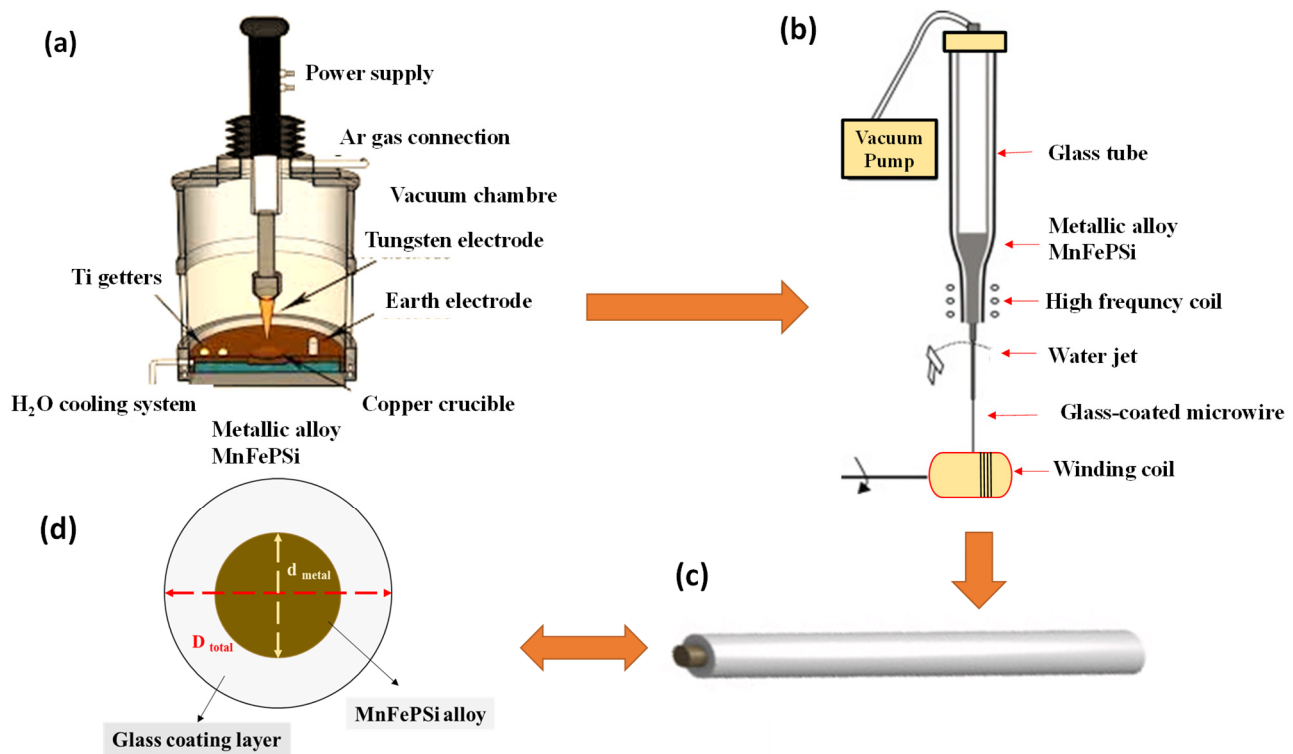


Figure 1. An image of the experimental setup facility for the fabrication of Mn–Fe–P–Si glass-coated microwires. (a) Vacuum ARC melting, (b) the Taylor–Ulitsky method for the production of glass-coated microwires, (c,d) the Mn–Fe–P–Si-based glass-coated microwires sketch.

2.3. Characterization of Structural and Magnetic Properties

Structural characterization of the samples was conducted using a (D8 Advance, Bruker AXS GmbH, Karlsruhe, Germany) X-ray diffractometer equipped with $\text{CuK}\alpha$ radiation at room temperature. A θ – 2θ scanning geometry with a step size of 0.02° and a range of 0° to 80° was employed.

Magnetic characterization was performed using a vibrating-sample magnetometer integrated within a Physical Property Measurement System (PPMS) (Quantum Design, San Diego, CA, USA). To characterize thermomagnetic behavior, magnetization was measured as temperature varied under a constant 50 Oe magnetic field, aligned with the microwire axis, within a 5 K to 400 K range. A ZFC-FC-FH procedure was employed: the sample was

cooled from 400 K without a field, then a 50 Oe field was applied, and magnetization was recorded during heating to 350 K (ZFC), followed by cooling to 5 K (FC), and subsequent heating to 350 K (FH), all at a 2 K/min rate. Hysteresis loops were also determined using a vibrating-sample magnetometer, applying magnetic fields up to 90 kOe along the wire axis, within a 5 K to 300 K temperature range. To facilitate comparison of results, all magnetic data were presented in terms of normalized magnetization (M/M_{sat} or $M/M_{5\text{K}}$), where M_{sat} (or $M_{5\text{K}}$) represents the magnetic moment measured at the saturation field or at 5 K, respectively. The Curie temperature was determined by identifying the minimum point of the first derivative of the magnetic moment-versus-temperature curves. It is imperative to note that all characterizations, including magnetic measurements, X-ray diffraction (XRD) analysis, and morphological investigations, were performed on the wire samples.

3. Results

3.1. Structure Characterizations

Figure 2 shows the X-ray diffraction (XRD) analysis conducted in as-prepared Mn–Fe–P–Si glass-coated microwires and those annealed at 973 K, 1073 K, and 1123 K for 1 h, revealing notable differences in their microstructural properties. All diffractograms exhibited a broad halo below $2\theta \approx 30^\circ$, attributed to the amorphous glass coating, as previously reported [34,67–79]. The as-prepared microwire exhibited three distinct microstructure phases, while annealed samples exhibited two phases. The predominant phase in all samples was Fe_2P with the space group P-62 m. A hexagonal Mn_5Si_3 phase ($P6_3/mcm$) was found as a secondary phase in the initial sample, and a cubic Fe_3Si phase (Fm-3 m) was present in both the initial and the 973 K annealed samples. Annealing the samples at higher temperatures, specifically 1073 K and 1123 K for one hour, resulted in the elimination of the hexagonal Mn_5Si_3 phase, and indicates that Mn atoms may fill Fe sites, leading to an increase in the cubic Fe_3Si phase content. It was observed that through annealing, the main Fe_2P phase in Mn–Fe–P–Si microwires increased, while the secondary phases diminished. For the samples annealed at 973 K and 1073 K for 1 h, increased peak intensities at 30° , 46.9° , 53.5° , and 65.3° 2θ confirmed a higher Fe_2P phase content. For the sample annealed at 1123 K for 1 h, only four peaks were observed, at $2\theta = 30^\circ$ (200, Fe_2P), $2\theta = 35.1^\circ$ (002, Fe_3Si), 46.3° (200, Fe_2P), and $2\theta = 53.5^\circ$ (200, Fe_2P). Analysis showed that the lattice parameter initially decreased with annealing at 973 K (from 0.58 ± 0.02 nm to 0.54 ± 0.02 nm) and then increased significantly at 1123 K (to 0.61 ± 0.02 nm, Table 1). These changes, along with phase formation, are linked to the observed variations in magnetic behavior, discussed later. Similarly, the average grain size increased from 36 nm (as-prepared) to 133 nm (973 K) and 147 nm (1123 K, Table 1), indicating a strong temperature dependence.

Table 1. Chemical composition, lattice constant, and average grain size of as-prepared Mn–Fe–P–Si-based glass-coated microwires and those annealed at different temperatures.

Samples	Chemical Composition	Lattice Constant (nm)	D_g (nm)
As-prepared	$\text{Mn}_{40}\text{Fe}_{30}\text{P}_{15}\text{Si}_{15}$	0.58	36
973 K (1 h)	$\text{Mn}_{40}\text{Fe}_{30}\text{P}_{15}\text{Si}_{15}$	0.54	136
1073 K (1 h)	$\text{Mn}_{40}\text{Fe}_{30}\text{P}_{15}\text{Si}_{15}$	0.60	141
1123 K (1 h)	$\text{Mn}_{40}\text{Fe}_{30}\text{P}_{15}\text{Si}_{15}$	0.61	148

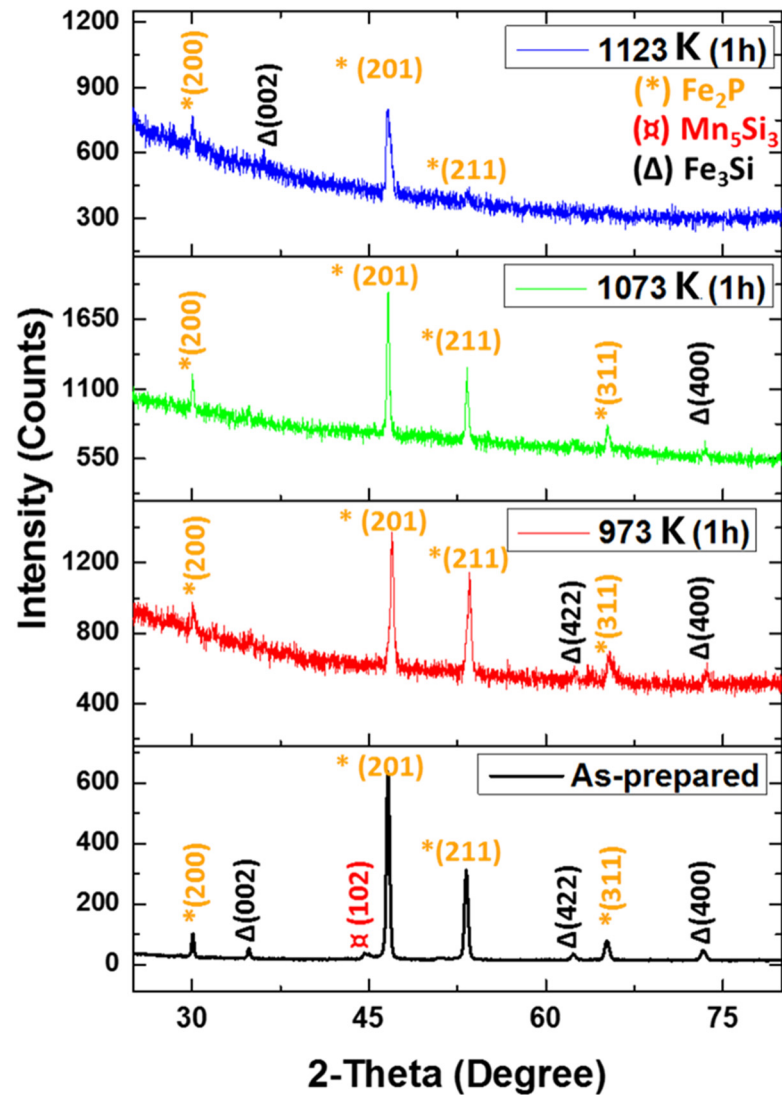


Figure 2. The X-ray diffraction profile measured at room temperature of as-prepared MnFePSi glass-coated microwires and those annealed at 973 K, 1073 K, and 1123 K for 1 h.

3.2. Magnetic Hysteresis Loops Characterization

Figure 3 summarizes the magnetic hysteresis loops of Mn–Fe–P–Si-based glass-coated microwire samples measured at 5 K. All magnetic measurements were performed in the in-plane configuration with the applied magnetic field aligned parallel to the wire axis, where the easy magnetization axis is expected. Annealing significantly altered the magnetic properties of the samples, as shown by magnetic measurements performed with the glass coating present. While the as-prepared sample displayed unsaturated hysteresis loops even at 90 kOe, the annealed samples exhibited saturated loops at fields below 5 kOe. This substantial change in saturation behavior, illustrated in Figure 3, demonstrates the effectiveness of annealing in modifying the magnetic characteristics of the material. Furthermore, the M-H loops of the untreated sample demonstrate multi-step magnetic behavior and unusual metamagnetic transition at a low temperature (see Figure 3b). Such unusual magnetic behavior is discussed in detail in our previous works [19,74–76]. For an annealed sample at 1123 K for 1 h, M-H loops exhibit an inclined shape that should be attributed to the micro-magnetic structure induced by a high-temperature annealing process. From Figure 3b, it can be seen that the sample annealed at 973 for 1 h exhibits stronger magnetic behavior with respect to the rest of the samples. Meanwhile, magnetic softening is observed in the sample annealed at 1123 K for 1 h.

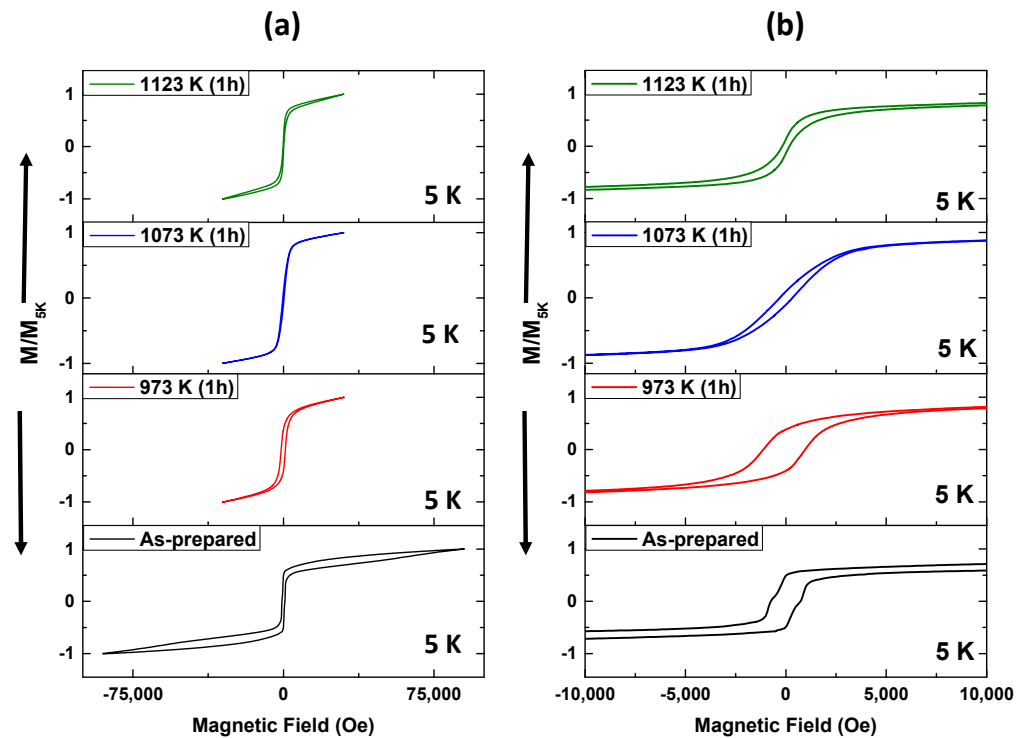


Figure 3. The in-plane hysteresis loops of as-prepared Mn–Fe–P–Si glass-coated microwires and those annealed at 973 K, 1073 K, and 1123 K for 1 h measured at 5 K at (a) the full measuring scale and (b) at a low scale.

Investigation the Mn–Fe–P–Si glass-coated microwire samples at room temperature, i.e., where $T \approx 300$ K, notably different magnetic behavior is seen compared to the samples measured at 5 K. First, the as-prepared samples exhibit regular magnetic behavior without any distortion in the magnetic hysteresis loop. In addition, magnetic softening is evidenced by the hysteresis loops measured at 300 K in low magnetic fields (see Figures 3b and 4b). Secondly, a notable reduction in the saturation field follows from complete saturation in a magnetic field below 5 kOe. The same behavior is seen in the annealed samples, in which the hysteresis loops measured at room temperature exhibit soft magnetic behavior compared to the loops measured at 5 K. The softest magnetic behavior is observed in the annealed sample at 1123 K for 1 h. In addition, a strong paramagnetic contribution is seen in the sample annealed at 1123 K, where the hysteresis loop has an almost linear shape (see Figure 4b).

Figure 5 illustrates the temperature dependence of coercivity (H_c) for both as-prepared and annealed Mn–Fe–P–Si glass-coated microwires. In general, the $H_c(T)$ dependencies are typical for ferromagnetic behavior; as the temperature drops from 300 K to 5 K, the coercive field H_c increases. A maximum coercive field (H_c) of around 1200 Oe at 5 K was achieved by the sample annealed at 973 K for 1 h, the highest among all the samples tested. For samples annealed at 1073 K and 1123 K, a notable reduction in H_c was observed, decreasing from 325 Oe to 150 Oe and from 175 Oe to 30 Oe, respectively, over the temperature range of 5 K to 300 K. This tunability of magnetic properties of Mn–Fe–P–Si glass-coated microwires by annealing can be attributed to the internal stress relaxation and the average grain size modification. The main origin of such internal stresses is the difference in thermal expansion coefficients of the glass coating and the metallic alloy [68,69,72]. Such internal stress relaxation can induce modifications in the microstructure and magnetic properties of the metallic nucleus.

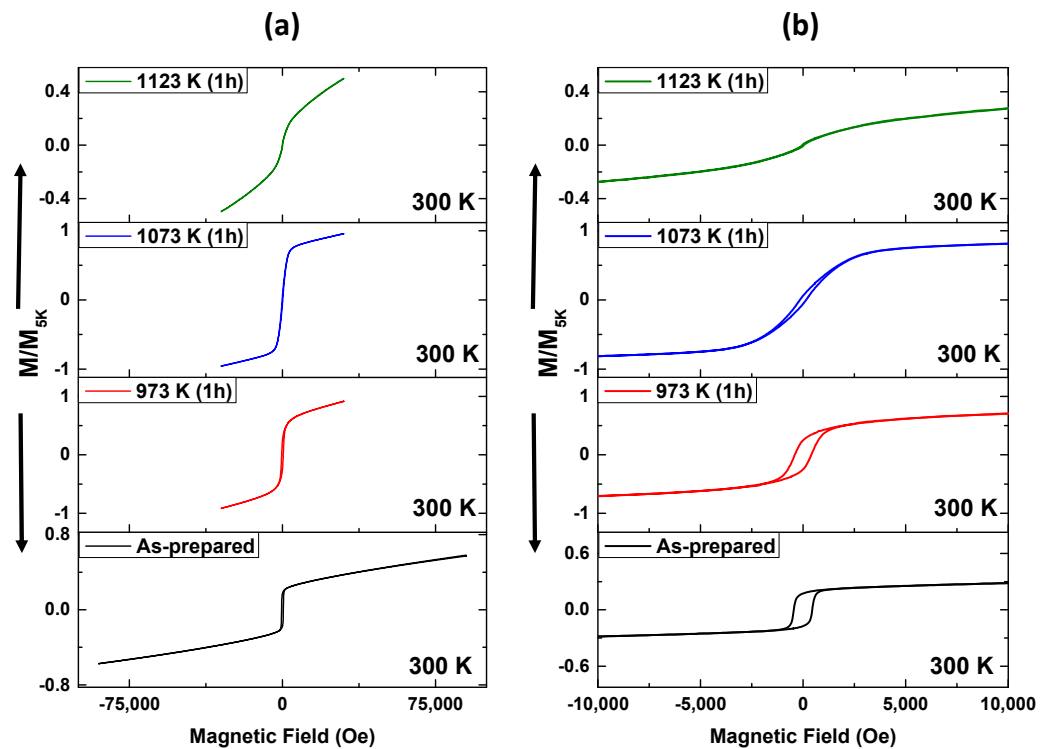


Figure 4. The hysteresis loops measured in the plane of the as-prepared Mn–Fe–P–Si glass-coated microwires and those annealed at 973 K, 1073 K, and 1123 K for (1 h) measured at 300 K (a) for the full measuring scale and (b) the low-field region.

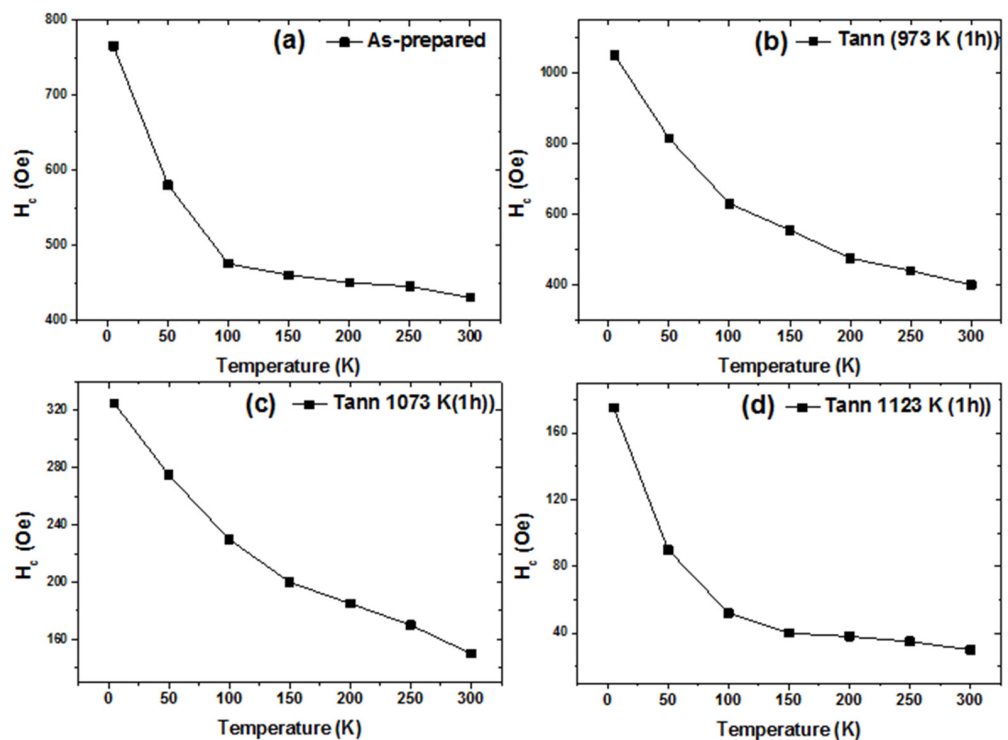


Figure 5. Temperature dependence of coercivity, H_c , in Mn–Fe–P–Si-based glass-coated microwire: (a) as-prepared, (b) annealed at 973 K for 1 h, (c) annealed at 1073 K for (1 h), and (d) 1123 K for (1 h).

The increase in grain size from 36 nm in as-prepared samples to ~140 nm in annealed samples suggests a possible transition from single-domain to multi-domain magnetization processes, which could influence coercivity and magnetization behavior. In addition, the reduction in H_c from 1200 Oe (annealed at 973 K) to 150 Oe (annealed at 1123 K) aligns

with the expected inverse relationship between coercivity and grain size ($H_c \sim 1/Dg$ for $Dg > 100$ nm) [77]. Furthermore, stress relaxation due to the difference in thermal expansion between the metallic core and the glass coating contributes to reduced domain wall pinning, allowing further magnetic softening.

While grain size plays an important role, the other factor affecting magnetic properties is the phase transformation, as evidenced by XRD analysis, which indicates an increase in the Fe_2P phase and a reduction in secondary phases. The Fe_2P phase exhibits strong magneto-crystalline anisotropy, significantly influencing coercivity and overall magnetic response.

Thus, while grain size increase facilitates domain wall motion and the internal stress relaxation provides magnetic softening, the drastic changes in coercivity and magnetic properties also correlate with the Fe_2P phase content evolution and the suppression of secondary phases. This correlation is supported by previous studies on nanocrystalline materials and Fe_2P -based alloys.

Therefore, the observed changes in the magnetic properties of Mn–Fe–P–Si glass-coated microwires upon annealing can be attributed to a combination of factors, including grain size evolution, phase transformations, and stress relaxation.

To gain insight into the magnetic behavior of Mn–Fe–P–Si glass-coated microwires, thermomagnetic characterization was performed. Magnetization was measured as a function of temperature (5–400 K) under constant magnetic fields of 1 kOe and 5 kOe (Figures 6 and 7), applied along the wire axis. An FC-FH protocol was used: cooling from 400 K without a field, applying the field and heating to 400 K, then cooling (FC) and reheating (FH), all at 2 K/min.

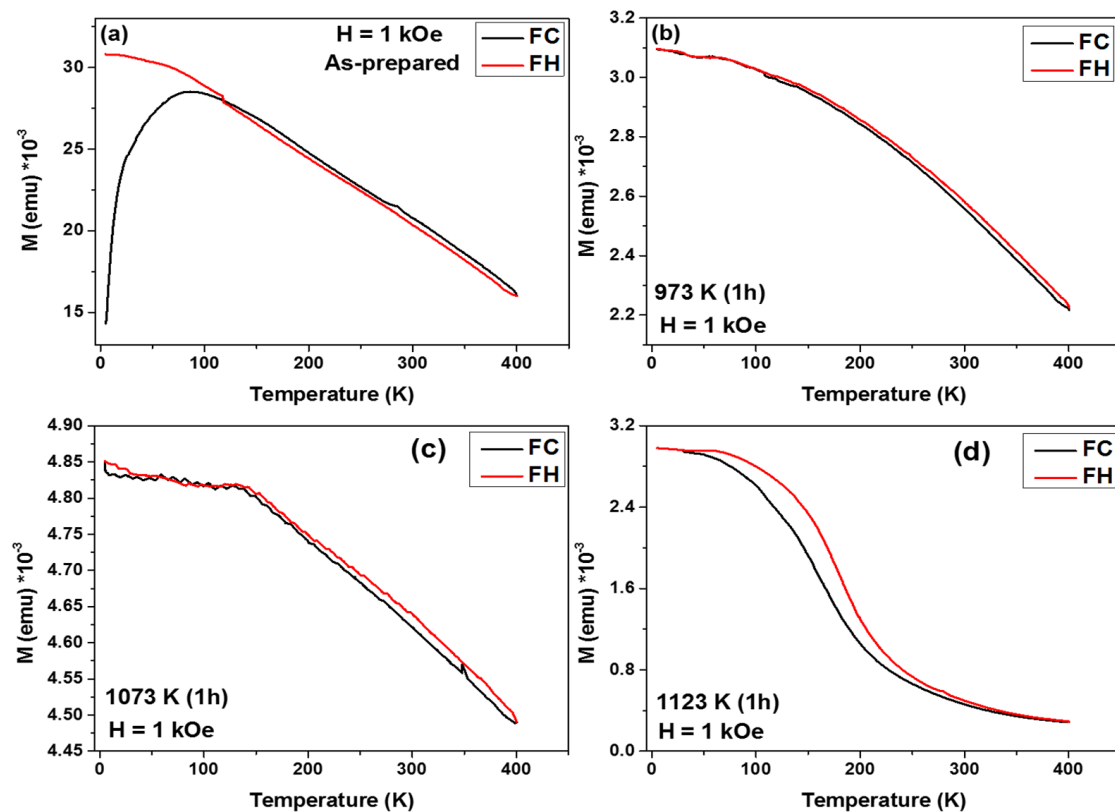


Figure 6. The temperature dependence of field-cooled (FC) and field-heated (FH) magnetization was measured at a magnetic field of 1 kOe for the as-prepared Mn–Fe–P–Si-based glass-coated microwire (a) and for samples annealed at different temperatures: 973 K for 1 h (b), 1073 K for 1 h (c), and 1123 K for 1 h (d).

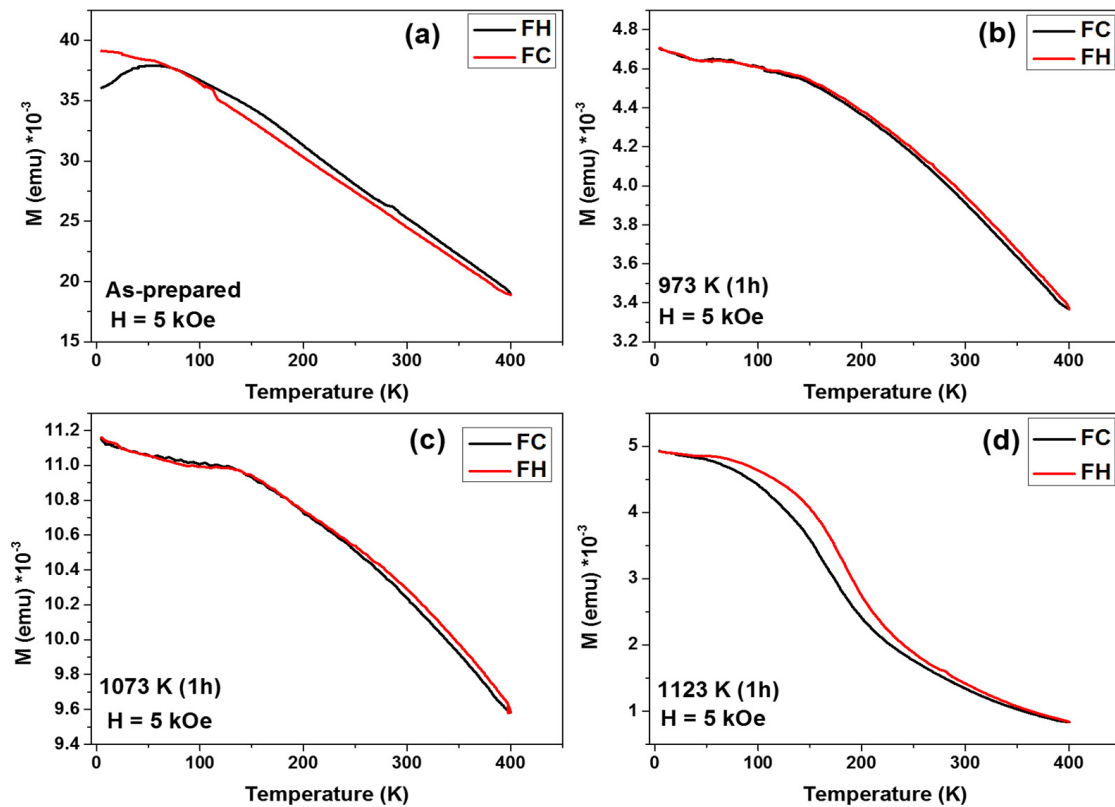


Figure 7. The temperature dependence of the field-cooled (FC) and field-heated (FH) magnetization of as-prepared Mn–Fe–P–Si-based glass-coated microwire (a) and that annealed at different temperatures ((b) 973 K (1 h), (c) 1073 K (1 h), and (d) 1123 K (1 h)) measured in a magnetic field ($H = 5$ kOe).

The FC curve for the as-prepared sample shows different behavior compared to the annealed samples. The FH curve perfectly matches with the FH of annealed samples. More details about the thermomagnetic behavior of the as-prepared sample are discussed in our previous works [19,74]. FC and FH curves for the annealed sample at 973 K show regular ferromagnetic behavior where the magnetization increases monotonically by decreasing the temperature from 400 K to 5 K. For the sample annealed at 1073 K, the same behavior is seen, but with two different slopes for $M(T)$ dependence: by decreasing the temperature, the magnetization rate is changed. This change in the magnetization rate and slopes is due to the existence of a secondary phase, as will be discussed in the XRD section. For the annealed sample at 1123 K for 1 h, notable hysteric behavior is observed, where the separation between FC and FH appears at a temperature range from 50 to 350 K. The hysteretic behavior indicates the common thermomagnetic behavior of the Fe_2P -based alloys. Thus, the annealing affects the thermomagnetic response of Mn–Fe–P–Si-based glass-coated microwires.

The observed changes in magnetic properties with temperature, including coercivity, field-cooled, and field-heated behaviors, are consistent with the confirmed link between microstructure and magnetism in thermal treatment samples. The minor variations in magnetic behavior within the annealed samples are likely due to internal stress and grain size effects on the micromagnetic structure. Additional research into the micromagnetic structure of these annealed samples is needed for a more comprehensive understanding.

Our findings suggest that annealing within the temperature range of 973 K to 1123 K for one hour induces recrystallization, grain size growth, atomic ordering, and causes a reduction in internal stresses within the microwires. These structural modifications contribute to the enhancement of the Fe_2P phase, which is responsible for the thermomag-

netic response of Mn–Fe–P–Si-based alloys. The appearance of two magnetic phases with differing magnetic anisotropies explains the unique magnetic behavior of the annealed Mn–Fe–P–Si glass-coated microwires.

4. Conclusions

Our research clearly indicates that annealing Mn–Fe–P–Si glass-coated microwires at high temperatures (973 K, 1073 K, and 1123 K) for an hour has a profound effect on their magnetic and microstructural properties. The annealing process results in a decrease in secondary phases found in the initial sample, an increase in the Fe₂P phase, and also facilitates grain size growth and the relaxation of internal stress. The combination of all these factors substantially affects the material's thermo-magnetic performance. Notably, hysteresis loop analysis reveals that annealing suppresses the metamagnetic phase transition and multistep magnetic behaviors observed in the as-prepared sample, promoting ferromagnetic ordering. This transformation results in a more homogeneous magnetic response with a significantly lower saturation field below 5 kOe compared to the 90 kOe observed in the as-prepared sample. Furthermore, the sample annealed at 973 K for 1 h exhibits the highest coercivity value, reaching approximately 1.2 kOe, while the lowest coercivity value is observed for the sample annealed at 1123 K for 1 h, which exhibits a value of around 30 Oe. Interestingly, the sample annealed at 1123 K for 1 h FC and FH curves demonstrate notable hysteretic behavior at a temperature range of 50–350 K. This study demonstrates that annealing is a powerful method to precisely control the magnetic properties of MnFePSi glass-coated microwires, opening up new possibilities for their use in various applications of glass-coated microwire technology.

Author Contributions: Conceptualization, M.S. and A.Z.; methodology, M.S. and V.Z.; validation, M.S., V.Z. and A.Z.; formal analysis, M.S.; investigation, M.S. and A.Z.; resources, J.G., V.Z. and A.Z.; data curation M.S. and V.Z.; writing—original draft preparation, M.S. and A.Z.; writing—review and editing, M.S. and A.Z.; visualization, M.S. and V.Z.; supervision, A.Z.; project administration, J.G., V.Z. and A.Z.; funding acquisition, J.G., V.Z. and A.Z. All authors have read and agreed to the published version of the manuscript.

Funding: The authors appreciate the technical and human support provided by SGIker of UPV/EHU and European funds (ERDF and ESF). The research was made possible by funding from the Spanish MICIN (project PID2022-141373NB-I00), EU Horizon Europe projects “INFINITE” and “Harmony”, Basque Government Elkartek projects “ATLANTIS” and “MOSINCO”, and the “Ayuda a Grupos Consolidados” grant (IT1670-22). M.S. acknowledges the Maria Zambrano contract funding from the Spanish Ministerio de Universidades and EU—Next Generation EU.

Data Availability Statement: The original contributions presented in this study are included in the article. Further inquiries can be directed to the corresponding authors.

Acknowledgments: The authors thank the technical and human support provided by SGIker of UPV/EHU (Medidas Magneticas Gipuzkoa) and European funding (ERDF and ESF).

Conflicts of Interest: The authors declare no conflicts of interest.

References

1. Hou, Y.L.; Sellmyer, D.J. *Magnetic Nanomaterials: Fundamentals, Synthesis and Applications*; John Wiley & Sons: New York, NY, USA, 2017; pp. 3–546.
2. Kitanovski, A. Energy applications of magnetocaloric materials. *Adv. Energy Mater.* **2020**, *10*, 1903741. [[CrossRef](#)]
3. Burch, K.S.; Mandrus, D.; Park, J.G. Magnetism in two-dimensional van der Waals materials. *Nature* **2018**, *563*, 47–52. [[CrossRef](#)] [[PubMed](#)]
4. Trevizoli, P.V.; Barbosa, J.R. Overview on magnetic refrigeration. In *Encyclopedia of Smart Materials*; Olabi, A., Ed.; Elsevier: Oxford, UK, 2022; pp. 395–406. [[CrossRef](#)]

5. Phan, M.H.; Yu, S.C. Review of the magnetocaloric effect in manganite materials. *J. Magn. Magn. Mater.* **2007**, *308*, 325–340. [[CrossRef](#)]
6. Salaheldeen, M.; Abu-Dief, A.M.; El-Dabea, T. Functionalization of Nanomaterials for Energy Storage and Hydrogen Production Applications. *Materials* **2025**, *18*, 768. [[CrossRef](#)]
7. Lu, A.H.; Salabas, E.L.; Schuth, F. Magnetic nanoparticles: Synthesis, protection, functionalization, and application. *Angew. Chem. Int. Ed.* **2007**, *46*, 1222–1244. [[CrossRef](#)]
8. Salaheldeen, M.; Zhukova, V.; Blanco, J.M.; Gonzalez, J.; Zhukov, A. The Impact of High-Temperature Annealing on Magnetic Properties, Structure and Martensitic Transformation of Ni₂MnGa-based Glass-Coated Microwires. *Ceram. Int.* **2025**, *51*, 4378–4387. [[CrossRef](#)]
9. Fernández-Pacheco, R.; Streubel, O.; Fruchart, O.; Hertel, R.; Fischer, P.; Cowburn, R.P. Three-dimensional nanomagnetism. *Nat. Commun.* **2017**, *8*, 15756. [[CrossRef](#)]
10. Moya, X.; Kar-Narayan, S.; Mathur, N.D. Caloric materials near ferroic phase transitions. *Nat. Mater.* **2014**, *13*, 439–450.
11. Wederni, A.; Salaheldeen, M.; Ipatov, M.; Zhukova, V.; Zhukov, A. Influence of the Geometrical Aspect Ratio on the Magneto-Structural Properties of Co₂MnSi Microwires. *Metals* **2023**, *13*, 1692. [[CrossRef](#)]
12. Manosa, L.; Planes, A. Materials with giant mechanocaloric effects: Cooling by strength. *Adv. Mater.* **2017**, *29*, 1603607.
13. Salaheldeen, M.; Wederni, A.; Ipatov, M.; Gonzalez, J.; Zhukova, V.; Zhukov, A. Elucidation of the Strong Effect of the Annealing and the Magnetic Field on the Magnetic Properties of Ni₂-Based Heusler Microwires. *Crystals* **2022**, *12*, 1755. [[CrossRef](#)]
14. Li, L.; Wu, Z.; Yuan, S.; Zhang, X.B. Advances and challenges for flexible energy storage and conversion devices and systems. *Energy Environ. Sci.* **2014**, *7*, 2101–2122. [[CrossRef](#)]
15. Alahmadi, M.; Mohamed, W.S.; Zhukov, A.; Salaheldeen, M.; Alsaedi, W.H.; Alhashmialameer, D.; Al-Ghamdi, K.; Abu Dief, A.M. One-step hydrothermal synthesis of flower-like MoS₂/VS₂ nanocomposite for biomedical applications. *Inorg. Chem. Commun.* **2023**, *157*, 111336. [[CrossRef](#)]
16. Salaheldeen, M.; Zhukova, V.; Ipatov, M.; Zhukov, A. GdFe-based nanostructured thin films with large perpendicular magnetic anisotropy for spintronic applications. *AIP Adv.* **2024**, *14*, 025308. [[CrossRef](#)]
17. Zhou, Y.; Zhao, X.; Xu, J.; Fang, Y.; Chen, G.; Song, Y.; Li, S.; Chen, J. Giant magnetoelastic effect in soft systems for bioelectronics. *Nat. Mater.* **2021**, *20*, 1670–1676. [[CrossRef](#)] [[PubMed](#)]
18. Bonnot, E.; Romero, R.; Manosa, L.; Vives, E.; Planes, A. Elastocaloric effect associated with the martensitic transition in shape-memory alloys. *Phys. Rev. Lett.* **2008**, *100*, 125901. [[CrossRef](#)]
19. Salaheldeen, M.; Vega, V.; Ibabe, A.; Jaafar, M.; Asenjo, A.; Fernandez, A.; Prida, V.M. Tailoring of Perpendicular Magnetic Anisotropy in Dy₁₃Fe₈₇ Thin Films with Hexagonal Antidot Lattice Nanostructure. *Nanomaterials* **2018**, *8*, 227. [[CrossRef](#)] [[PubMed](#)]
20. Salaheldeen, M.; Zhukova, V.; Gonzalez, J.; Zhukov, A. Anomalous magnetic behavior in MnFePSi glass-coated microwires. *J. Alloys Compd.* **2024**, *1002*, 175244. [[CrossRef](#)]
21. Hu, J.M.; Nan, C.W. Opportunities and challenges for magnetoelectric devices. *APL Mater.* **2019**, *7*, 080905. [[CrossRef](#)]
22. Liu, J.; Gottschall, T.; Skokov, K.P.; Moore, J.D.; Gutfleisch, O. Giant magnetocaloric effect driven by structural transitions. *Nat. Mater.* **2012**, *11*, 620–626. [[CrossRef](#)]
23. Salaheldeen, M.; Abu-Dief, A.M.; Martínez-Goyeneche, L.; Alzahrani, S.O.; Alkhatib, F.; Álvarez-Alonso, P.; Blanco, J.A. Dependence of the Magnetization Process on the Thickness of Fe₇₀Pd₃₀ Nanostructured Thin Film. *Materials* **2020**, *13*, 5788. [[CrossRef](#)] [[PubMed](#)]
24. Cong, D.Y.; Huang, L.; Hardy, V.; Bourgault, D.; Sun, X.M.; Nie, Z.H.; Wang, M.G.; Ren, Y.; Entel, P.; Wang, Y.D. Low-field-actuated giant magnetocaloric effect and excellent mechanical properties in a NiMn-based multiferroic alloy. *Acta Mater.* **2018**, *146*, 142–151.
25. Salaheldeen, M.; Talaat, A.; Ipatov, M.; Zhukova, V.; Zhukov, A. Preparation and Magneto-Structural Investigation of Nanocrystalline CoMn-Based Heusler Alloy Glass-Coated Microwires. *Processes* **2022**, *10*, 2248. [[CrossRef](#)]
26. Narita, F.; Fox, M. A review on piezoelectric, magnetostrictive, and magnetoelectric materials and device technologies for energy harvesting applications. *Adv. Eng. Mater.* **2018**, *20*, 1700743. [[CrossRef](#)]
27. Wu, Y.F.; Xuan, H.C.; Agarwal, S.; Xu, Y.K.; Zhang, T.; Feng, L.; Li, H.; Han, P.D.; Zhang, C.L.; Wang, D.H.; et al. Large magnetocaloric effect and magnetoresistance in Fe and Co co-doped Ni-Mn-Al Heusler alloys. *Phys. Status Solidi A* **2018**, *215*, 1700843.
28. Franco, V.; Blázquez, J.S.; Ipus, J.J.; Law, J.Y.; Moreno-Ramírez, L.M.; Conde, A. Magnetocaloric effect: From materials research to refrigeration devices. *Prog. Mater. Sci.* **2018**, *93*, 112–232.
29. Salaheldeen, M.; Zhukova, V.; Lopez Anton, R.; Zhukov, A. Dependence of Magnetic Properties of As-Prepared Nanocrystalline Ni₂MnGa Glass-Coated Microwires on the Geometrical Aspect Ratio. *Sensors* **2024**, *24*, 3692. [[CrossRef](#)]
30. Graf, T.; Parkin, S.S.P.; Felser, C. Heusler Compounds—A Material Class with Exceptional Properties. *IEEE Trans. Magn.* **2011**, *47*, 367–373.
31. Otsuka, K.; Wayman, C.M. *Shape Memory Materials*; Cambridge University Press: Cambridge, UK, 1999.

32. Salaheldeen, M.; Zhukova, V.; Ipatov, M.; Zhukov, A. Unveiling the Magnetic and Structural Properties of (X_2YZ ; $X = \text{Co}$ and Ni , $Y = \text{Fe}$ and Mn , and $Z = \text{Si}$) Full-Heusler Alloy Microwires with Fixed Geometrical Parameters. *Crystals* **2023**, *13*, 1550. [[CrossRef](#)]
33. Pushin, V.G. Alloys with a Termomechanical Memory: Structure, properties and application. *Phys. Met. Metallogr.* **2000**, *90* (Suppl. S1), S68–S95.
34. Cesare, R.; Pons, J.; Santamarta, R.; Segui, C.; Chernenko, V.A. Ferromagnetic Shape Memory Alloys: An Overview. *Arch. Metall. Mater.* **2004**, *49*, 779–789.
35. Salaheldeen, M.; Wederni, A.; Ipatov, M.; Zhukova, V.; Zhukov, A. Carbon-Doped Co_2MnSi Heusler Alloy Microwires with Improved Thermal Characteristics of Magnetization for Multifunctional Applications. *Materials* **2023**, *16*, 5333. [[CrossRef](#)] [[PubMed](#)]
36. Gschneidner, K.A.; Pecharsky, V.K. Thirty years of near room temperature magnetic cooling: Where we are today and future prospects. *Int. J. Refrig.* **2008**, *31*, 945–961. [[CrossRef](#)]
37. Smith, A.; Bahl, C.R.H.; Björk, R.; Engelbrecht, K.; Nielsen, K.K.; Pryds, N. Materials challenges for high performance magnetocaloric refrigeration devices. *Adv. Energy Mater.* **2012**, *2*, 1288–1318. [[CrossRef](#)]
38. Kuz'Min, M.D. Factors limiting the operation frequency of magnetic refrigerators. *Appl. Phys. Lett.* **2007**, *90*, 251916. [[CrossRef](#)]
39. Vuarnoz, D.; Kawanami, T. Numerical analysis of a reciprocating active magnetic regenerator made of gadolinium wires. *Appl. Therm. Eng.* **2012**, *37*, 388–395. [[CrossRef](#)]
40. Zhukov, A.; Ipatov, M.; del Val, J.J.; Zhukova, V.; Chernenko, V.A. Magnetic and structural properties of glass-coated Heusler-type microwires exhibiting martensitic transformation. *Sci. Rep.* **2018**, *8*, 621. [[CrossRef](#)]
41. Miao, X.F.; Hu, S.Y.; Xu, F.; Brück, E. Overview of magnetoelastic coupling in $(\text{Mn, Fe})_2(\text{P, Si})$ -type magnetocaloric materials. *Rare Met.* **2018**, *37*, 723–733. [[CrossRef](#)]
42. Gottschall, T.; Skokov, K.P.; Fries, M.; Taubel, A.; Radulov, I.; Scheibel, F.; Benke, D.; Riegg, S.; Gutfleisch, O. Making a cool choice: The materials library of magnetic refrigeration. *Adv. Energy Mater.* **2019**, *9*, 1901322. [[CrossRef](#)]
43. Suye, B.; Yibole, H.; Guillou, F. Influence of the particle size on a $\text{MnFe}(\text{P, Si, B})$ compound with giant magnetocaloric effect. *AIP Adv.* **2023**, *13*, 025203. [[CrossRef](#)]
44. Dung, N.H.; Zhang, L.; Ou, Z.Q.; Brück, E. From first-order magneto-elastic to magneto-structural transition in $(\text{Mn, Fe})_{1.95}\text{P}_{0.50}\text{Si}_{0.50}$ compounds. *Appl. Phys. Lett.* **2011**, *99*, 092511. [[CrossRef](#)]
45. Hudl, M.; Nordblad, P.; Björkman, T.; Eriksson, O.; Häggström, L.; Sahlberg, M.; Andersson, Y.; Delczeg-Czirjak, E.K.; Vitos, L. Order-disorder induced magnetic structures of $\text{FeMnP}_{0.75}\text{Si}_{0.25}$. *Phys. Rev. B* **2011**, *83*, 134420. [[CrossRef](#)]
46. Miao, X.F.; Caron, L.; Roy, P.; Dung, N.H.; Zhang, L.; Kockelmann, W.A.; de Groot, R.A.; van Dijk, N.H.; Brück, E. Tuning the phase transition in transition-metal-based magnetocaloric compounds. *Phys. Rev. B* **2014**, *89*, 174429. [[CrossRef](#)]
47. Ou, Z.Q.; Zhang, L.; Dung, N.H.; Caron, L.; Brück, E. Structure, magnetism and magnetocalorics of Fe-rich $(\text{Mn, Fe})_{1.95}\text{P}_{1-x}\text{Si}_x$ melt-spun ribbons. *J. Alloys Compd.* **2017**, *710*, 446e51. [[CrossRef](#)]
48. Dung, N.H.; Ou, Z.Q.; Caron, L.; Zhang, L.; Thanh, D.T.C.; de Wijs, G.A.; de Groot, R.A.; Buschow, K.H.J.; Brück, E. Mixed magnetism for refrigeration and energy conversion. *Adv. Energy Mater.* **2011**, *1*, 1215. [[CrossRef](#)]
49. Neish, M.J.; Oxley, M.P.; Guo, J.; Sales, B.C.; Allen, L.J.; Chisholm, M.F. Local Observation of the Site Occupancy of Mn in a MnFePSi Compound. *Phys. Rev. Lett.* **2015**, *114*, 106101. [[CrossRef](#)] [[PubMed](#)]
50. Miao, X.F.; Caron, L.; Gercsi, Z.; Daoud-Aladine, A.; van Dijk, N.H.; Brück, E. Thermal-history dependent magnetoelastic transition in $(\text{Mn, Fe})_2(\text{P, Si})$. *Appl. Phys. Lett.* **2015**, *107*, 042403. [[CrossRef](#)]
51. Zhang, F.; Smits, S.; Kiecana, A.; Batashev, I.; Shen, Q.; van Dijk, N.; Brück, E. Impact of W doping on Fe-rich $(\text{Mn, Fe})_2(\text{P, Si})$ based giant magnetocaloric materials. *J. Alloys Compd.* **2023**, *933*, 167802. [[CrossRef](#)]
52. Zheng, Z.; Wang, H.; Li, C.; Chen, X.; Zeng, D.; Yuan, S. Enhancement of magnetic properties and magnetocaloric effects for $\text{Mn}_{0.975}\text{Fe}_{0.975}\text{P}_{0.5}\text{Si}_{0.5}$ alloys by optimizing quenching temperature. *Adv. Energy Mater.* **2022**, *25*, 2200160. [[CrossRef](#)]
53. He, A.; Svitlyk, V.; Mozharivskyj, Y. Synthetic approach for $(\text{Mn, Fe})_2(\text{Si, P})$ magnetocaloric materials: Purity, structural, magnetic, and magnetocaloric properties. *Inorg. Chem.* **2017**, *56*, 2827–2833. [[CrossRef](#)]
54. Lai, J.; Huang, B.; You, X.; Maschek, M.; Zhou, G.; van Dijk, N.; Brück, E. Giant magnetocaloric effect for $(\text{Mn, Fe, V})_2(\text{P, Si})$ alloys with low hysteresis. *J. Sci. Adv. Mater. Dev.* **2024**, *9*, 100660. [[CrossRef](#)]
55. Miao, X.F.; Caron, L.; Gubbens, P.C.M.; Yaouanc, A.; de R'etotier, P.D.; Luetkens, H.; Amato, A.; van Dijk, N.H.; Brück, E. Spin correlations in $(\text{Mn, Fe})_2(\text{P, Si})$ magnetocaloric compounds above Curie temperature. *J. Sci. Adv. Mater. Dev.* **2016**, *1*, 147–151. [[CrossRef](#)]
56. Salaheldeen, M.; Zhukova, V.; Rosero-Romo, J.J.; Ipatov, M.; Zhukov, A. Preparation and magnetic properties of MnFePSi -based glass-coated microwires. *AIP Adv.* **2024**, *1*, 015350.
57. Zhang, H.; Gimaev, R.; Kovalev, B.; Kamilov, K.; Zverev, V.; Tishin, A. Review on the Materials and Devices for Magnetic Refrigeration in the Temperature Range of Nitrogen and Hydrogen Liquefaction. *Phys. B Condens. Matter* **2019**, *558*, 65–73.
58. Lai, J.; You, X.; Dugulan, I.; Huang, B.; Liu, J.; Maschek, M.; van Eijck, L.; van Dijk, N.; Brück, E. Tuning the magneto-elastic transition of $(\text{Mn, Fe, V})_2(\text{P, Si})$ alloys to low magnetic field applications. *J. Alloys Compd.* **2020**, *821*, 153451.

59. Lai, J.; Tang, X.; Sepehri-Amin, H.; Hono, K. Tuning transition temperature of magnetocaloric $\text{Mn}_{1.8}\text{Fe}_{0.2}(\text{P}_{0.59}\text{Si}_{0.41})_x$ alloys for cryogenic magnetic refrigeration. *Scr. Mater.* **2020**, *183*, 127–132.
60. Fries, M.; Pfeuffer, L.; Bruder, E.; Gottschall, T.; Ener, S.; Diop, L.V.B.; Gröb, T.; Skokov, K.P.; Gutfleisch, O. Microstructural and magnetic properties of Mn-Fe-P-Si (Fe_2P -type) magnetocaloric compounds. *Acta Mater.* **2017**, *132*, 222–229.
61. Tu, D.; Yan, J.; Xie, Y.; Li, J.; Feng, S.; Xia, M.; Li, J.; Leung, A.P. Accelerated design for magnetocaloric performance in Mn-Fe-P-Si compounds using machine learning. *J. Mater. Sci. Technol.* **2022**, *96*, 241–247.
62. Guillou, F.; Porcari, G.; Yibole, H.; van Dijk, N.H.; Bruck, E. Taming the first-order transition in giant magnetocaloric materials. *Adv. Mater.* **2014**, *26*, 2671–2675.
63. Dung, N.H.; Zhang, L.; Ou, Z.Q.; Zhao, L.; van Eijck, L.; Mulders, A.M.; Avdeev, M.; Suard, E.; van Dijk, N.H.; Bruck, E. High/low-moment phase transition in hexagonal Mn-Fe-P-Si compounds. *Phys. Rev. B* **2012**, *86*, 045134. [[CrossRef](#)]
64. Salaheldeen, M.; Zhukova, V.; Zhukov, A. Unraveling the impact of annealing and magnetic field on MnFePSi microwires. *J. Appl. Phys.* **2024**, *136*, 133902. [[CrossRef](#)]
65. Tu, D.; Li, J.; Zhang, R.; Hu, Q.; Li, J. Microstructure evolution, solidification characteristic and magnetocaloric properties of $\text{MnFeP}_{0.5}\text{Si}_{0.5}$ particles by droplet melting. *Intermetallics* **2021**, *131*, 107102. [[CrossRef](#)]
66. Yue, M.; Xu, M.F.; Zhang, H.G.; Zhang, D.T.; Liu, D.M.; Altounian, Z. Structural and magnetocaloric properties of $\text{MnFeP}_{1-x}\text{Si}_x$ compounds prepared by spark plasma sintering. *IEEE Trans. Magn.* **2015**, *51*, 2504804. [[CrossRef](#)]
67. Salaheldeen, M.; Zhukova, V.; Rosero, J.; Salazar, D.; Zhukov, A. Annealing-induced softening and metamagnetic transition control in MnFePSi microwires. *Intermetallics* **2025**, *181*, 108742. [[CrossRef](#)]
68. Salaheldeen, M.; Ipatov, M.; Zhukova, V.; García-Gomez, A.; Gonzalez, J.; Zhukov, A. Preparation and magnetic properties of CO_2 -based Heusler alloy glass-coated microwires with high Curie temperature. *AIP Adv.* **2023**, *13*, 025325. [[CrossRef](#)]
69. Salaheldeen, M.; Ipatov, M.; Corte-Leon, P.; Zhukova, V.; Zhukov, A. Effect of Annealing on the Magnetic Properties of Co_2MnSi -Based Heusler Alloy Glass-Coated Microwires. *Metals* **2023**, *13*, 412. [[CrossRef](#)]
70. Chiriac, H.; Ovari, T.A. Amorphous glass-covered magnetic wires: Preparation, properties, applications. *Prog. Mater. Sci.* **1996**, *40*, 333–407. [[CrossRef](#)]
71. Salaheldeen, M.; Wederni, A.; Ipatov, M.; Zhukova, V.; Zhukov, A. Preparation and Magneto-Structural Investigation of High-Ordered (L_{21} Structure) Co_2MnGe Microwires. *Processes* **2023**, *11*, 1138. [[CrossRef](#)]
72. Salaheldeen, M.; Garcia-Gomez, A.; Ipatov, M.; Corte-Leon, P.; Zhukova, V.; Blanco, J.M.; Zhukov, A. Fabrication and Magneto-Structural Properties of Co_2 -Based Heusler Alloy Glass-Coated Microwires with High Curie Temperature. *Chemosensors* **2022**, *10*, 225. [[CrossRef](#)]
73. Zhukova, V.; Cobeño, A.F.; Zhukov, A.; Blanco, J.M.; Larin, V.; Gonzalez, J. Coercivity of glass-coated $\text{Fe}_{73.4-x}\text{Cu}_1\text{Nb}_{3.1}\text{Si}_{13.4+x}\text{B}_{9.1}$ ($0 \leq x \leq 1.6$) microwires. *Nanostruct. Mater.* **1999**, *11*, 1319–1327. [[CrossRef](#)]
74. Salaheldeen, M.; Wederni, A.; Ipatov, M.; Zhukova, V.; Lopez Anton, R.; Zhukov, A. Enhancing the Squareness and Bi-Phase Magnetic Switching of Co_2FeSi Microwires for Sensing Application. *Sensors* **2023**, *23*, 5109. [[CrossRef](#)] [[PubMed](#)]
75. Salaheldeen, M.; Zhukova, V.; Rosero, J.; Salazar, D.; Ipatov, M.; Zhukov, A. Comparison of the magnetic and structural properties of MnFePSi microwires and MnFePSi bulk alloy. *Materials* **2024**, *17*, 1874. [[CrossRef](#)]
76. Vázquez, M. Soft magnetic wires. *Phys. B Condens. Matter* **2001**, *299*, 302–313.
77. Salaheldeen, M.; Garcia-Gomez, A.; Corte-Leon, P.; Gonzalez, A.; Ipatov, M.; Zhukova, V.; Lopez Anton, R.; Zhukov, A. Manipulation of magnetic and structure properties of Ni_2FeSi glass-coated microwires by annealing. *J. Alloys Compd.* **2023**, *942*, 169026. [[CrossRef](#)]
78. López Antón, R.; Andres, J.P.; Gonzalez, J.A.; Garcia-Gomez, A.; Zhukova, V.; Chizhik, A.; Salaheldeen, M.; Zhukov, A. Tuning of magnetic properties and Giant Magnetoimpedance effect in multilayered microwires. *J. Sci. Adv. Mater. Devices* **2024**, *9*, 100821. [[CrossRef](#)]
79. Herzer, G. Modern soft magnets: Amorphous and nanocrystalline materials. *Acta Mater.* **2013**, *61*, 718–734.

Disclaimer/Publisher’s Note: The statements, opinions and data contained in all publications are solely those of the individual author(s) and contributor(s) and not of MDPI and/or the editor(s). MDPI and/or the editor(s) disclaim responsibility for any injury to people or property resulting from any ideas, methods, instructions or products referred to in the content.